AD-A116 562

AD #-116 562

TECHNICAL REPORT ARLCB-TR-82012

TECHNICAL LIBRARY

THE COMBINED EFFECTS OF MEAN STRESS AND AGGRESSIVE ENVIRONMENTS ON FATIGUE CRACK GROWTH

J. A. Kapp

May 1982

US ARMY ARMAMENT RESEARCH AND DEVELOPMENT COMMAND
LARGE CALIBER WEAPON SYSTEMS LABORATORY
BENÉT WEAPONS LABORATORY
WATERVLIET, N. Y. 12189

AMCMS No. 61110191A0011

DA Project No. 1L161101A9A

PRON No. 1A2231491A1A

APPROVED FOR PUBLIC RELEASE; DISTRIBUTION UNLIMITED

DISCLAIMER

The findings in this report are not to be construed as an official Department of the Army position unless so designated by other authorized documents.

The use of trade name(s) and/or manufacture(s) does not constitute an official indorsement or approval.

DISPOSITION

Destroy this report when it is no longer needed. Do not return it to the originator.

SECURITY CLASSIFICATION OF THIS PAGE *(When Data Entered)*

REPORT DOCUMENTATION PAGE

READ INSTRUCTIONS BEFORE COMPLETING FORM

1. REPORT NUMBER: ARLCB-TR-82012	2. GOVT ACCESSION NO.
3. RECIPIENT'S CATALOG NUMBER	
4. TITLE *(and Subtitle)*: THE COMBINED EFFECTS OF MEAN STRESS AND AGGRESSIVE ENVIRONMENTS ON FATIGUE CRACK GROWTH	5. TYPE OF REPORT & PERIOD COVERED: Final
	6. PERFORMING ORG. REPORT NUMBER
7. AUTHOR(s): J. A. Kapp	8. CONTRACT OR GRANT NUMBER(s)
9. PERFORMING ORGANIZATION NAME AND ADDRESS: US Army Armament Research & Development Command, Benet Weapons Laboratory, DRDAR-LCB-TL, Watervliet, NY 12189	10. PROGRAM ELEMENT, PROJECT, TASK AREA & WORK UNIT NUMBERS: AMCMS No. 61110191A0011, DA Project No. 1L161101A9A, PRON No. 1A2231491A1A
11. CONTROLLING OFFICE NAME AND ADDRESS: US Army Armament Research & Development Command, Large Caliber Weapon Systems Laboratory, Dover, NJ 07801	12. REPORT DATE: May 1982
	13. NUMBER OF PAGES: 20
14. MONITORING AGENCY NAME & ADDRESS *(if different from Controlling Office)*	15. SECURITY CLASS. *(of this report)*: UNCLASSIFIED
	15a. DECLASSIFICATION/DOWNGRADING SCHEDULE

16. DISTRIBUTION STATEMENT *(of this Report)*

Approved for public release; distribution unlimited.

17. DISTRIBUTION STATEMENT *(of the abstract entered in Block 20, if different from Report)*

18. SUPPLEMENTARY NOTES

Presented at 1982 Joint JSME-SESA Conference on Experimental Mechanics, Honolulu, HI, 23-30 May 1982.
Published in proceedings of the conference.

19. KEY WORDS *(Continue on reverse side if necessary and identify by block number)*

Fatigue Crack Growth
Mean Stress Effects
Liquid Metal Embrittlement
Fracture Mechanics

20. ABSTRACT *(Continue on reverse side if necessary and identify by block number)*

Experiments have been performed to study the combined effects of aggressive environment and mean stress on fatigue crack growth. Since mean stress changes also change the stress ratio, $R(R = \sigma_{min}/\sigma_{max})$, experiments were performed to measure fatigue crack growth rates for various values of constant R. The experimental results were approximated mathematically using a modified superposition model. The results show that for negative values of R, the

(CONT'D ON REVERSE)

DD FORM 1 JAN 73 1473 EDITION OF 1 NOV 65 IS OBSOLETE

UNCLASSIFIED

SECURITY CLASSIFICATION OF THIS PAGE *(When Data Entered)*

20. ABSTRACT (CONT'D)

modified superposition model yields excellent agreement with the experiments. When R was positive, the mathematical model significantly overestimated the experimental results, suggesting that the full environmental effect condition cannot be achieved in the embrittling system chosen. By including a factor to account for the less than 100 percent environmental effect, excellent agreement between the model and the experimental results was obtained when R was positive. Throughout the study, a high strength, low alloy steel embrittled by liquid mercury was used.

TABLE OF CONTENTS

LIST OF ILLUSTRATIONS

INTRODUCTION

One of the applications of studying mean stress effects in fatigue is residual stress. Often in the manufacture of engineering structures residual stresses are induced in the structure either intentionally or inadvertently. Examples of the former are shot peened automotive components, swaged holes in aircraft skins or autofrettaged thick cylinders. Falling into the latter category are welded structures or certain heat treated components with complex geometries. When such a component is subjected to fatigue, its life can either be extended or decreased depending on the sense of the residual stress. Normally compressive stresses result in enhanced life while tensile stresses usually accelerate failure. Much work has been done to study the effects of residual stress on fatigue[1] in inert environments. If the additional variable of aggressive environment is included, things become even more complex. To this author's knowledge, no organized study has been undertaken to address this problem.

Although no work has been published dealing exclusively with the residual stress aspect of corrosion fatigue crack growth, much work has been conducted to study the basic phenomena.[2] Fatigue crack growth in aggressive environments is influenced by many factors including loading frequency, waveform, temperature, and mean stress or stress ratio R ($R = \sigma_{min}/\sigma_{max}$). Of these, the R effect is that factor which is related to residual stresses. This aspect of

---

[1]Throop, J. F., Report to ASTM Committee E-9 on the Formation of Subcommittee E09.02 on Residual Stress Effects in Fatigue," Philadelphia, PA, November 1980.

[2]Wei, R. P., in Fatigue Mechanisms, Jeffrey T. Fong, ASTM STP 675, ASTM, Philadelphia, PA, 1979, p. 816.

environmentally enhanced fatigue crack growth is the subject of this report.

The aggressive environment system used to study these effects was liquid mercury and a low alloy high strength steel. It is well known that liquid mercury very strongly attacks steels to cause liquid metal embrittlement (LME).[3] Although not a commonly occurring embrittlement system in industry, the system is very similar to the hydrogen-steel system. It will be shown that crack growth in mercury follows the same shaped curve as the hydrogen-steel curve[2] and the magnitude of crack growth rate is also about the same. Using mercury thus provides a good analogy to a practical system without the expense of special testing chambers and equipment.

We will show the results of tests performed at various values of constant R. A model will then be proposed to mathematically fit the data. Shortcomings of the model will be discussed suggesting that the full effect of the environmental interaction cannot be attained.

EXPERIMENTAL PROCEDURE

The basic experiments involved in the testing reported herein are the measurement of crack growth rates in the environment under controlled R conditions. It was decided to use pure bending samples, since these can be used to very easily produce controlled R testing conditions and are easily manufactured.

---

[2]Wei, R. P., in Fatigue Mechanisms, Jeffrey T. Fong, ASTM STP 675, ASTM, Philadelphia, PA, 1979, p. 816.

[3]Stoloff, N. S., in Environment Sensitive Fracture of Engineering Materials, Z. A. Foroulis, Ed., The Metallurgical Society of AIME, New York, 1979, p. 486.

Since we were concerned with only the R value effect, the initial experiments were performed at constant waveform, loading frequency, and temperature. These conditions were sine wave at 30 Hz at room temperature. Five R conditions were tested, R = ± 0.6, ± 0.3, and 0.0. In a cracked body R is determined as the ratio of stress intensity factors, K, rather than the ratio of stresses, ($R = K_{min}/K_{max}$). The subscripts refer to the minimum and maximum K respectively that occurs during the fatigue cycle. Figure 1 shows the bend sample which was used to measure the fatigue crack growth rates. The K solution for this specimen is well known and the expression for K as a function of loading conditions and crack depth is given as:[4]

$$K = \frac{4M}{B/W^{3/2}} \cdot f(a/W)$$

$$f(a/W) = \frac{3(a/W)^{1/2}}{2(1+2a/W)(1-a/W)^{3/2}} (1.99 - a/W(1-a/W) \times (2.15 - 3.93\ a/W + 2.7(a/W)^2)) \quad (1)$$

where M is the applied moment, and a, B, and W are the crack length thicknesses shown in Figure 1.

---

[4]Srawley, J. E., International J. of Fracture Mechanics, Vol. 12, June 1976, p. 475.

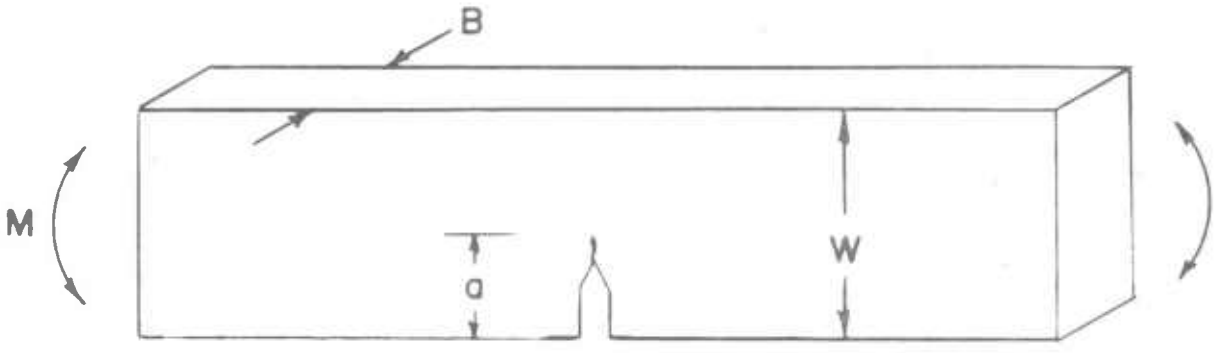

Figure 1. Schematic Representation of the Bend Specimen Used

All of the variables in Eq. (1) were fixed once the testing commenced except for the crack length, a. To measure crack growth in aggressive environments several methods have been used. In this study we used the crack mouth opening displacement (CMOD) method.[5] Using the technique, the CMOD is continuously measured. With all other variables fixed, as the crack grows, the CMOD increases. Expressions similar in form to Eq. (1), relating CMOD and the other loading and specimen variables for many specimens, are presently being developed.[6] For the specimen considered here, the expression is:

$$a/W = \delta'(-0.980 + 5.150\delta' - 4.288\delta'^{2} + 1.11\delta'^{3})$$

$$\delta' = \frac{1}{1 + \left(\frac{15.8M}{(\Delta CMOD)EBW}\right)^{1/2}} \qquad (2)$$

where E is Young's modulus of the material, and ΔCMOD is the range of CMOD measured in the experiments. Equation (2) is accurate to within ± one percent for any value of δ'.

The specimens were prepared such that LME was produced. This requires that two criteria be met:[3] (1) intimate contact between the liquid metal and the solid metal, and (2) tensile stresses at the crack tip. The first criterion is more difficult to obtain since wetting must occur. Steel is very

---

[3]Stoloff, N. S., in Environment Sensitive Fracture of Engineering Materials, Z. A. Foroulis, Ed., The Metallurgical Society of AIME, New York, 1979, p. 486.

[5]Yoder, G. R. and Crooker, T. W., "The Procedure for Precision Measurement and Analyzing Fatigue Crack Growth Using Crack Opening for Corrosion Fatigue," presented at ASTM E-9 Symposium, Pittsburgh, PA, 1979.

[6]Kapp, J. A. and Newman, J. C. Jr., and Gross, B., in progress.

difficult to wet with liquid mercury. To alleviate this, the specimens were first plated with a thin copper coating which can be wetted very easily with mercury. The specimens were then fatigue loaded to break the copper coating and develop fatigue cracks in the steel beneath. Since freshly created crack surfaces are very clean, wetting occurs easily. In this way we were able to produce embrittlement quite readily. The steel used was gun steel heat treated to a yield strength of about 1170 MPa.

MATHEMATICAL MODEL OF EMBRITTLED CRACK GROWTH

Crack growth in inert environments in the steel tested follows the well known Paris power law:[7]

$$\left(\frac{da}{dN}\right)_{inert} = C\Delta K^m \qquad (3)$$

where $(da/dN)_{inert}$ is the crack growth rate, ΔK is the range of stress intensity factor, and C and m are empirical constants. It has been suggested[8] that the total fatigue crack growth, $(da/dN)_{total}$, in an aggressive environment can be modeled as:

$$(da/dN)_{total} = (da/dN)_{inert} + (da/dN)_{envir} \qquad (4)$$

where $(da/dN)_{envir}$ is the contribution of the aggressive environment which can be approximated based on the sustained load stress corrosion cracking behavior of the material in the environment considered.

---

[7]Paris, P. C. and Erdogan, F., Trans. ASME, Vol. 85, 1963, p. 528.
[8]Wei, R. P. and Landes, J. D., Mat. Res. Std., Vol. 9, 1969, p. 25.

Using Eq. (4) we are able to develop a model for crack growth in an aggressive environment which incorporates the effects of R values. Consider the idealized sustained loading crack growth response in Figure 2. If the applied K is below some critical value, K_{ISCC}, no crack growth occurs. When K exceeds K_{ISCC}, the crack grows at a constant velocity, v*, until the fracture toughness, K_{Ic} is reached at which point unstable fracture occurs. If we assume that $da/dN)_{environ}$ is totally accounted for by this property of the environment-metal system, this term can easily be determined on a cycle by cycle basis. For one cycle, the component of fatigue crack growth is given as

$$\frac{da}{dN})envir = v^* \times (\text{that period of time that K exceeds } K_{ISCC}) \qquad (5)$$

To determine the period of time that K exceeds K_{ISCC} in any single cycle, Figure 3 is useful. Referring to the figure, the time at which K equals K_{ISCC} is t*. The amount of time which K exceeds K_{ISCC} is then twice the amount $(\pi-t^*)/2\pi f$, where f is the frequency in Hz. Thus Eq. (5) becomes

$$\left(\frac{da}{dN}\right)_{envir} = \frac{v^*(\pi-t^*)}{\pi f} \qquad (6)$$

The value of t* must be calculated to determine the environmental contribution. To do this it is first necessary to get the expression for K as a function time in terms of the variables ΔK and R. Referring again to Figure 3 we find that for one cycle at one Hz

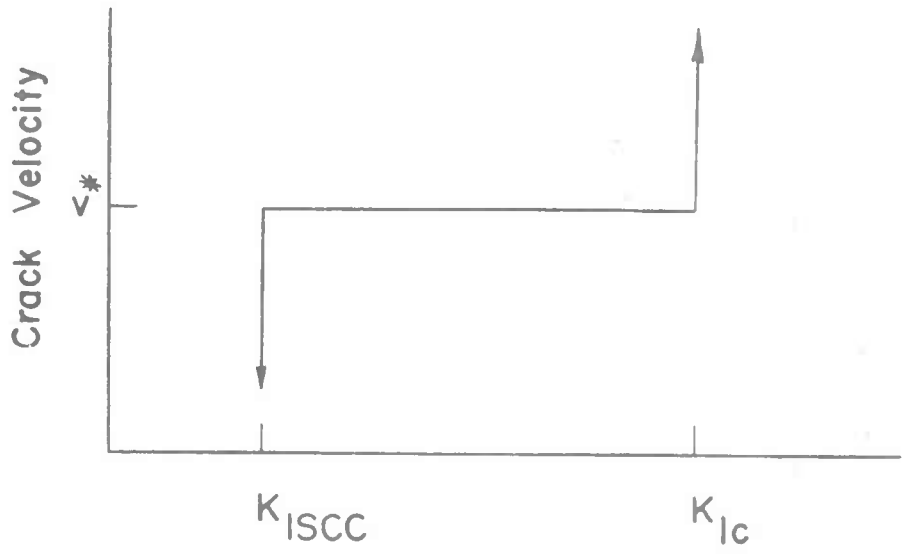

Figure 2. The Idealized Sustained Load Crack Velocity Property

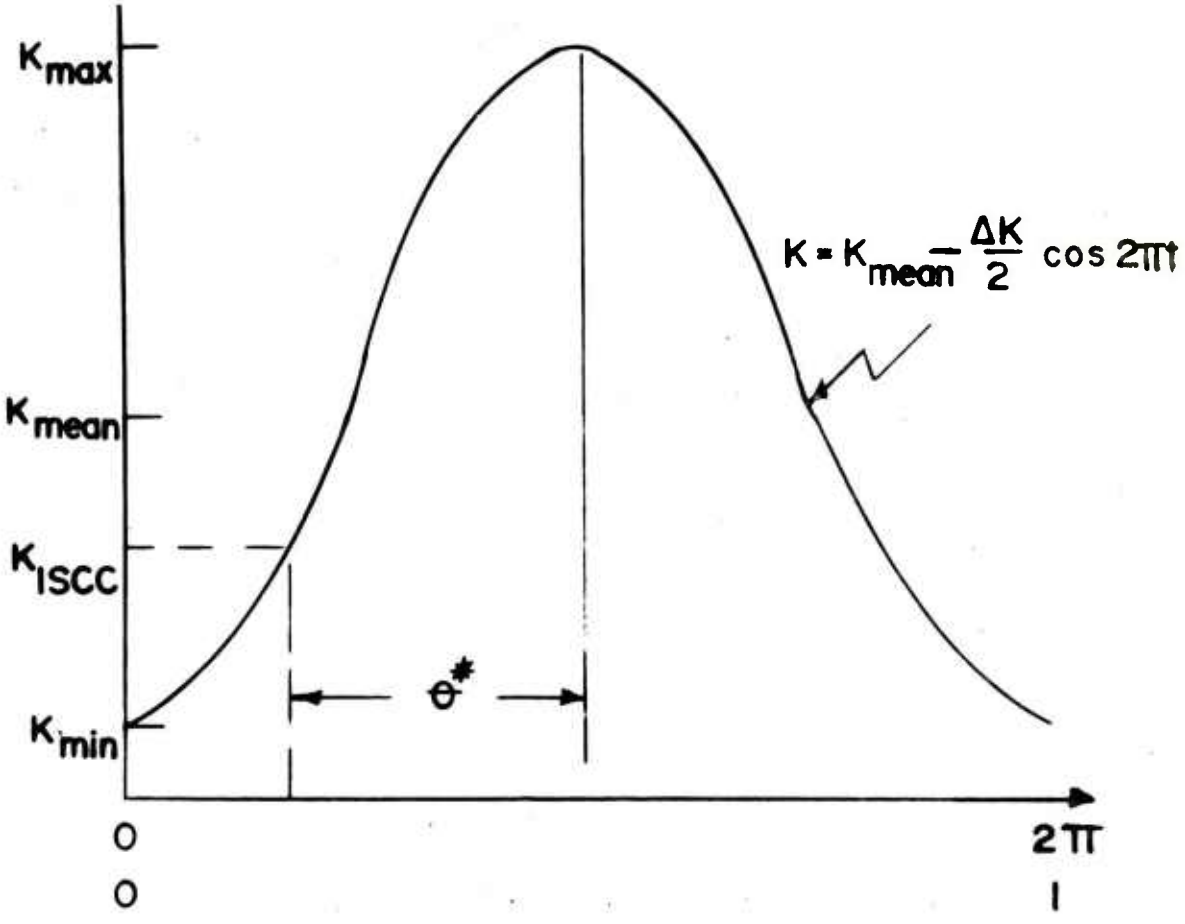

Figure 3. One Sinusoidal Fatigue Cycle

$$K(t) = \frac{\Delta K}{2} \cos 2\pi t + K_{mean} \tag{7}$$

$$K_{mean} = \frac{1}{2}(K_{max}+K_{min})$$

$$\Delta K = K_{max} - K_{min}$$

$$R = \frac{K_{min}}{K_{max}}$$

It can be easily determined that

$$K_{max} = \frac{\Delta K}{(1-R)} \tag{8}$$

$$K_{min} = \frac{R\Delta K}{(1-R)} \tag{9}$$

$$K_{mean} = \frac{\Delta K}{2}\left(\frac{1+R}{1-R}\right) \tag{10}$$

Using Eq. (10), Eq. (7) becomes

$$K(t) = \frac{\Delta K}{2}\left(\frac{1+R}{1-R} - \cos 2\pi t\right) \tag{11}$$

When $K(t) = K_{ISCC}$, t has the value t*, corresponding to $\Theta = \Theta^* = 2\pi t^*$, making Eq. (11)

$$K(t^*) = K_{ISCC} = \frac{\Delta K}{2}\left(\frac{1+R}{1-R} - \cos \Theta^*\right) \tag{12}$$

Solving for Θ^*, Eq. (12) becomes

$$\Theta^* = \arccos\left\{\frac{(1+R)}{(1-R)} - \frac{2K_{ISCC}}{\Delta K}\right\} \tag{13}$$

The time at which K exceeds K_{ISCC} is

$$\text{time} = \frac{1}{f} \times \frac{2(\pi-\Theta^*)}{2\pi} \tag{14}$$

Combining Eqs. (13) and (14)

$$\text{time that K exceeds } K_{ISCC} = [1 - \frac{1}{\pi} \arccos\{\frac{(1+R)}{(1-R)} - \frac{2K_{ISCC}}{\Delta K}\}] \qquad (15)$$

Combining Eqs. (15) and (6) the environmental component of fatigue crack growth is

$$\left(\frac{da}{dN}\right)_{envir} = \frac{v^*}{f} [1 - \frac{1}{\pi} \arccos[\frac{(1+R)}{(1-R)} - \frac{2K_{ISCC}}{\Delta K}]] \qquad (16)$$

There are some conditions which are applied to Eq. (15) to make it valid. If the maximum K occurring during the fatigue cycle is less than K_{ISCC}, there is no environmental contribution. Furthermore, if the minimum K during the fatigue cycle is greater than K_{ISCC}, there is always an environmental effect. This corresponds to $t^* = 0$. Under this condition the environmental component is easily obtained from Eq. (6) by setting $t^* = 0$. Realizing these facts and using Eqs. (8) and (9) for limits, the total crack growth rate, Eq. (4) can be written as:

$$\frac{da}{dN} = \begin{cases} C\Delta K^m & \frac{\Delta K}{(1-R)} \leq K_{ISCC} \\ C\Delta K^m + \frac{v^*}{f} [1 - \frac{1}{\pi} \arccos[\frac{(1+R)}{(1-R)} - \frac{2K_{ISCC}}{\Delta K}]] & \frac{R\Delta K}{(1-R)} \leq K_{ISCC} \leq \frac{\Delta K}{(1-R)} \\ C\Delta K^m + \frac{v^*}{f} & K_{ISCC} \leq \frac{R\Delta K}{(1-R)} \end{cases} \qquad (17)$$

Using this equation to model the combined effects of aggressive environment and stress ratio has several advantages. If it indeed applies, there are two material properties which need be found to explain the data, the velocity, v*, and K_{ISCC}. This being the case, only one set of experiments, in theory, need be performed in order to develop the crack growth rate property. Also, using an equation of this type, crack growth predictions can be made quite easily by numerical integration. The major drawback is that it applies for only one waveform, sinusoidal.

RESULTS AND DISCUSSION

The crack growth rate results for five different constant values of R (0, ± 0.3, ± 0.6) are shown in Figure 4. The straight line is the inert environment property of the material tested, which has been previously developed.[9] The curved lines are fit to the data, using Eq. (17). Several comments about the data can be made.

It is apparent from the actual measurement of crack growth rate that the threshold ΔK for accelerated crack growth increases with decreasing R value. This result conforms the assumption of a threshold K_{ISCC}, which is basic to the formulation of the crack growth model. If we use the R = 0 as a base, K_{ISCC} would be that value of ΔK where deviation from the inert environment behavior is observed. For the data in Figure 4, this value is about 33 $MPa\sqrt{m}$. Eq. (17) predicts that accelerated crack growth would occur for non-zero

---

[9]Underwood, J. H. and Throop, J. F., Part-Through Crack Fatigue Life Prediction, ASTM STP 687, J. B. Chang, Ed., ASTM, Philadelphia, PA, 1979, p. 195.

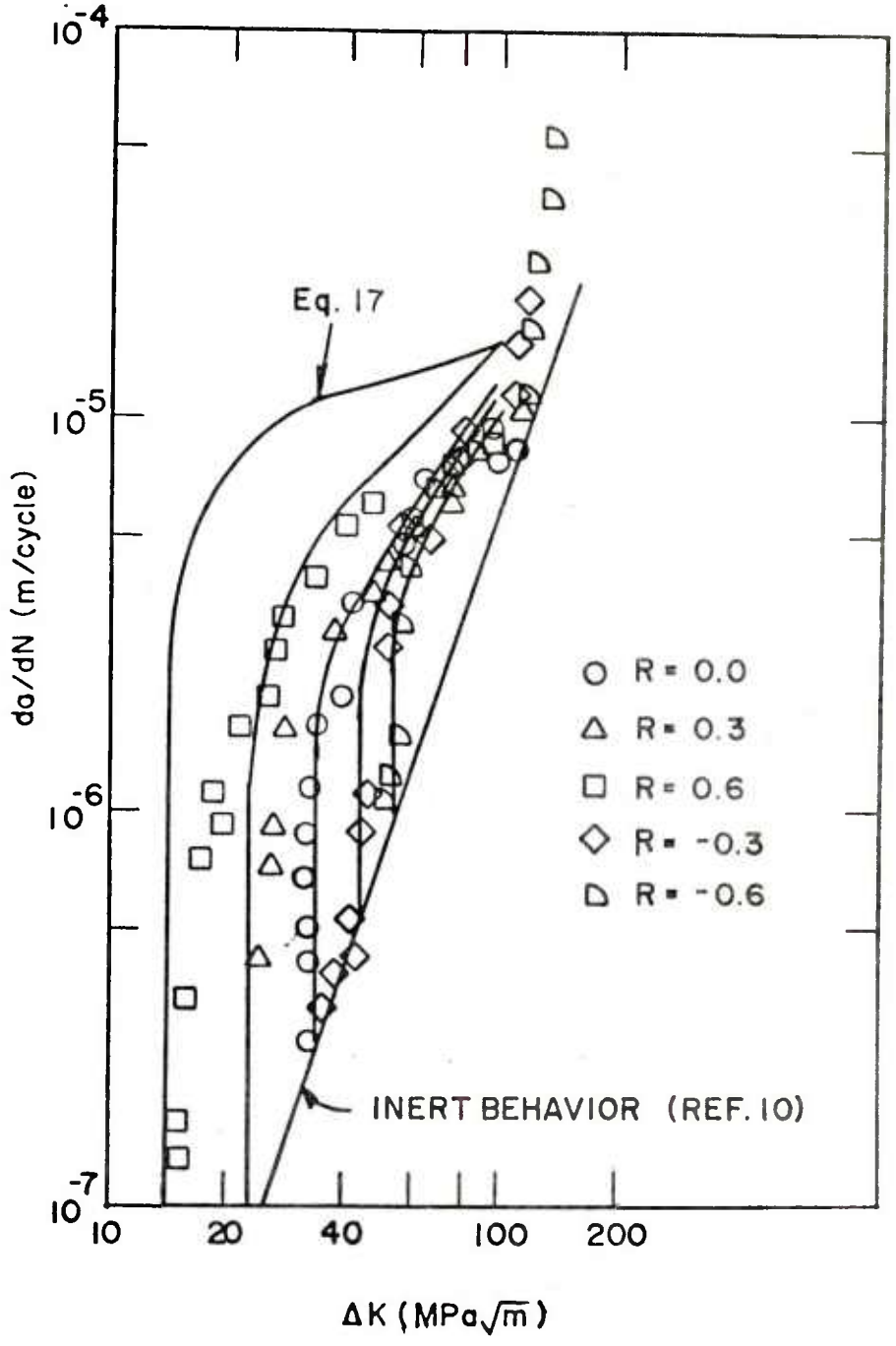

Figure 4. Comparison of the Measured Results with the Uncorrected Model

R values when $\Delta K = 33(1-R)$. For R of +0.6, +0.3, and -0.6, the critical ΔK values are calculated as 13, 23, 33, 43, and 53 MPa$\sqrt{m}$, respectively. The actual critical ΔK values for the respective R values tested were 15, 25, 33, 44, and 53 MPa$\sqrt{m}$. This is excellent agreement.

The crack growth behavior beyond the critical ΔK value, phenomenologically, can be explained as follows. As ΔK increases, da/dN increases very rapidly over a short range of ΔK. Increasing ΔK further, the increase in da/dN is much more gradual, until at some very high ΔK value, in this case about 100 MPa$\sqrt{m}$, there seems to be little effect of the aggressive environment.

The general shape of the observed behavior is well characterized by the proposed model. Eq. (17) shows that there should be a limit to environmental effect, when $\Delta K > K_{ISCC}(1-R)/R$, while the inert, Paris power law component always increases with ΔK. This indicates that there could be some value of ΔK, at which the environmental component of embrittlement becomes insignificant. The model predicts this limiting behavior quite well for negative values of R tested.

When R is positive, the maximum crack growth rate at high ΔK values is overestimated, using Eq. (17). In this case, it is possible for K to exceed K_{ISCC} for the entire fatigue cycle. The model proposed by Eq. (17) suggests under these conditions that the crack is always growing at the velocity v* from the environment, in addition to the crack growth from the inert fatigue conditions. The actual experimental results shown in Figure 4 suggest that there is a limit to the amount of environmental interaction which occurs regardless of R value. Please note how all the data converge to a crack

growth rate of about 10^{-5} m/cycle at ΔK of about 100 MPa$\sqrt{m}$. Equation (17) predicts that at ΔK of 100 MPa$\sqrt{m}$ the crack growth rate approaches 1.6×10^{-5} m/cycle for either positive R value testing condition. This suggests that only about 63 percent of the full environmental effect was actually attained in the experiment.

The overestimation of the actual behavior also occurs when a partial environmental effect is expected. For example, consider the R = +0.3 condition at ΔK of about 50 MPa$\sqrt{m}$. The total crack growth rate, given by Eq. (16) is about 7×10^{-6} m/cycle. The inert component is 8.15×10^{-7} m/cycle and the environmental component is 6.185×10^{-6} m/cycle. If the environmental component is reduced to 63 percent of the predicted value, the total crack growth rate would be 4.7×10^{-6} m/cycle. In the experiment, the crack growth rate measured was about 4.4×10^{-6} m/cycle, which agrees quite well with the predicted value. Therefore, a better fit to the actual data is suggested as follows:

$$\frac{da}{dN} = \begin{cases} C\Delta K^m & \Delta K \leq (1-R)K_{ISCC} \\ C\Delta K^m + \dfrac{Av^*}{f}\left[1 - \dfrac{1}{\pi}\arccos\left\{\dfrac{(1+R)}{(1-R)} - \dfrac{2K_{ISCC}}{\Delta K}\right\}\right] & (1-R)K_{ISCC} \leq \Delta K \leq \dfrac{(1-R)}{R}K_{ISCC} \\ C\Delta K^m + \dfrac{Av^*}{f} & \Delta K \geq \dfrac{(1-R)}{R}K_{ISCC} \end{cases} \qquad (18)$$

where

$$A = \begin{cases} 1.0 & R \leq 0 \\ 0.63 & R \leq 0 \end{cases}$$

$$C = 6.52 \times 10^{-12}$$

$$m = 3$$

$$f = 30 \text{ Hz}$$

$$K_{ISCC} = 33 \text{ MPa}\sqrt{m}$$

Using Eq. (18), the actual observed data is compared with theory in Figure 5 showing much better agreement.

The reasons for this type of behavior at positive R values are not immediately apparent. A possible explanation may be an inability of the liquid metal to access the crack tip for embrittlement to take place. Gordon[10] has suggested that the rate of crack growth in liquid metal embrittlement may be limited by the flow of liquid metal in capillary created by the newly created fracture surfaces. Using fluid mechanics, an equation was derived which related the fluid velocity (V_f) to the separation of the fracture surfaces, approximated as the crack tip opening displacement (CTOD):

$$V_f = (CTOD)^2 \cdot f(\text{solid metal-liquid properties, crack length}) \quad (19)$$

Under static loading condition, CTOD is a function of the yield strength of the solid metal and applied K. If, under the cyclic fatigue conditions studied here we consider the CTOD to be an RMS value for a sine wave, the $CTOD_{RMS}$ is about 0.707 of the maximum CTOD. Therefore, the fluid flow according to Eq. (19) under cyclic loading would be 0.5 of the CTOD under

---

[10]Gordon, P., Met. Trans. A., Vol. 9A, 1970, p. 614.

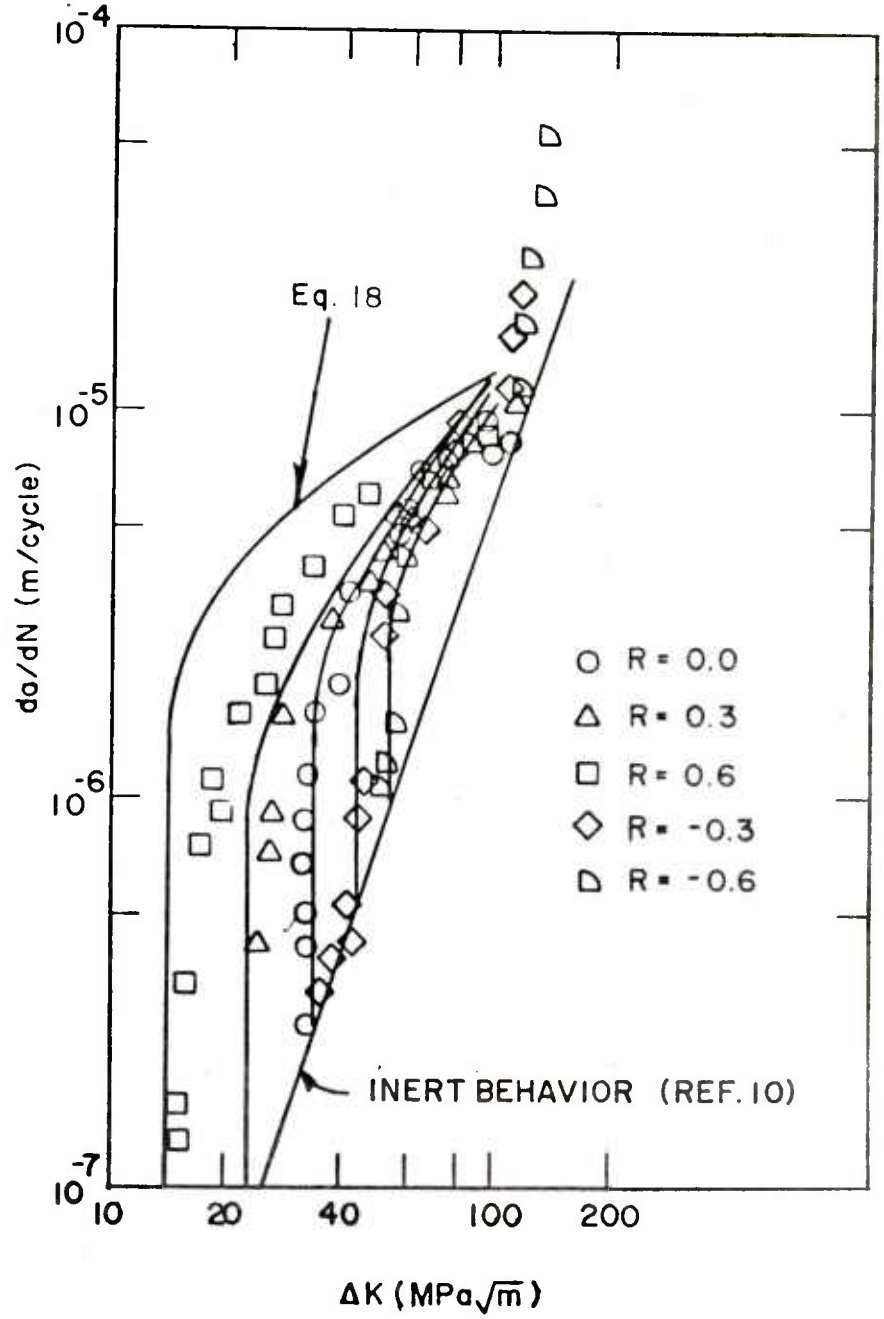

Figure 5. Comparison of the Measured Results with the Modified Model

static conditions. If it is assumed that the fluid velocity limits the crack growth rate, the above analysis suggests that only about 50 percent of the full environmental effect could be attained. From the experimental data, it was found that about 63 percent of the full environmental effect was observed. This comparison suggests that the fluctuating nature of the crack tip opening displacement may account for the need for correction factors in the model when R is positive. It also may suggest that this effect may be needed when R is negative because the waveform is also sinusoidal in these cases and the CTOD is certainly changing. In such instances only a portion of the fatigue cycle is above the K_{ISCC}, and the environmental interaction can only occur during that portion of the cycle when K is greater than K_{ISCC}. Under these circumstances, the CTOD does not change as much as when the entire cycle is above K_{ISCC}. Thus, the correction from the model should be less in the cases when R is negative.

CONCLUSIONS

The effect of mean stress or R ratio on fatigue crack growth in an aggressive environment has been measured. The crack growth rates can be accounted for very effectively by a simple superposition model when R is zero or negative. A correction must be made to the model when R is positive. The justification for the correction factor is the restriction of the environmental access to the crack tip from cyclic loading.

REFERENCES

1. Throop, J. F., "Report to ASTM Committee E-9 on the Formation of Subcommittee E09.02 on Residual Stress Effects in Fatigue," Philadelphia, PA, November 1980.
2. Wei, R. P., in Fatigue Mechanisms, Jeffrey T. Fong, Ed., ASTM STP 675, ASTM, Philadelphia, PA, 1979, p. 816.
3. Stoloff, N. S., in Environment Sensitive Fracture of Engineering Materials, Z. A. Foroulis, Ed., The Metallurgical Society of AIME, New York, 1979, p. 486.
4. Srawley, J. E., International J. of Fracture Mechanics, Vol. 12, June 1976, p. 475.
5. Yoder, G. R. and Crooker, T. W., "The Procedure for Precision Measurement and Analyzing Fatigue Crack Growth Using Crack Opening for Corrosion Fatigue," Presented at ASTM E-9 Symposium, Pittsburgh, PA, 1979.
6. Kapp, J. A. and Newman, J. C., Jr., and Gross, B., in progress.
7. Paris, P. C. and Erdogan, F., Trans. ASME, Vol. 85, 1963, p. 528.
8. Wei, R. P. and Landes, J. D., Mat. Res. Std., Vol. 9, 1969, p. 25.
9. Underwood, J. H. and Throop, J. F., Part-Through Crack Fatigue Life Prediction, ASTM STP 687, J. B. Chang, Ed., ASTM, Philadelphia, PA, 1979, p. 195.
10. Gordon, P., Met. Trans. A., Vol. 9A, 1970, p. 614.

TECHNICAL REPORT INTERNAL DISTRIBUTION LIST

	NO. OF COPIES
COMMANDER	1
CHIEF, DEVELOPMENT ENGINEERING BRANCH	1
ATTN: DRDAR-LCB-DA	1
-DM	1
-DP	1
-DR	1
-DS (SYSTEMS)	1
-DS (ICAS GROUP)	1
-DC	1
CHIEF, ENGINEERING SUPPORT BRANCH	1
ATTN: DRDAR-LCB-SE	1
-SA	1
CHIEF, RESEARCH BRANCH	2
ATTN: DRDAR-LCB-RA	1
-RC	1
-RM	1
-RP	1
TECHNICAL LIBRARY	5
ATTN: DRDAR-LCB-TL	
TECHNICAL PUBLICATIONS & EDITING UNIT	2
ATTN: DRDAR-LCB-TL	
DIRECTOR, OPERATIONS DIRECTORATE	1
DIRECTOR, PROCUREMENT DIRECTORATE	1
DIRECTOR, PRODUCT ASSURANCE DIRECTORATE	1

NOTE: PLEASE NOTIFY DIRECTOR, BENET WEAPONS LABORATORY, ATTN: DRDAR-LCB-TL, OF ANY REQUIRED CHANGES.

TECHNICAL REPORT EXTERNAL DISTRIBUTION LIST

	NO. OF COPIES
ASST SEC OF THE ARMY RESEARCH & DEVELOPMENT ATTN: DEP FOR SCI & TECH THE PENTAGON WASHINGTON, D.C. 20315	1
COMMANDER US ARMY MAT DEV & READ. COMD ATTN: DRCDE 5001 EISENHOWER AVE ALEXANDRIA, VA 22333	1
COMMANDER US ARMY ARRADCOM ATTN: DRDAR-LC -LCA (PLASTICS TECH EVAL CEN) -LCE -LCM -LCS -LCW -TSS (STINFO) DOVER, NJ 07801	1 1 1 1 1 1 2
COMMANDER US ARMY ARRCOM ATTN: DRSAR-LEP-L ROCK ISLAND ARSENAL ROCK ISLAND, IL 61299	1
DIRECTOR US ARMY BALLISTIC RESEARCH LABORATORY ATTN: DRDAR-TSB-S (STINFO) ABERDEEN PROVING GROUND, MD 21005	1
COMMANDER US ARMY ELECTRONICS COMD ATTN: TECH LIB FT MONMOUTH, NJ 07703	1
COMMANDER US ARMY MOBILITY EQUIP R&D COMD ATTN: TECH LIB FT BELVOIR, VA 22060	1
COMMANDER US ARMY TANK-AUTMV R&D COMD ATTN: TECH LIB - DRDTA-UL MAT LAB - DRDTA-RK WARREN, MICHIGAN 48090	1 1
COMMANDER US MILITARY ACADEMY ATTN: CHMN, MECH ENGR DEPT WEST POINT, NY 10996	1
US ARMY MISSILE COMD REDSTONE SCIENTIFIC INFO CEN ATTN: DOCUMENTS SECT, BLDG 4484 REDSTONE ARSENAL, AL 35898	2
COMMANDER REDSTONE ARSENAL ATTN: DRSMI-RRS -RSM ALABAMA 35809	1 1
COMMANDER ROCK ISLAND ARSENAL ATTN: SARRI-ENM (MAT SCI DIV) ROCK ISLAND, IL 61299	1
COMMANDER HQ, US ARMY AVN SCH ATTN: OFC OF THE LIBRARIAN FT RUCKER, ALABAMA 36362	1
COMMANDER US ARMY FGN SCIENCE & TECH CEN ATTN: DRXST-SD 220 7TH STREET, N.E. CHARLOTTESVILLE, VA 22901	1
COMMANDER US ARMY MATERIALS & MECHANICS RESEARCH CENTER ATTN: TECH LIB - DRXMR-PL WATERTOWN, MASS 02172	2

NOTE: PLEASE NOTIFY COMMANDER, ARRADCOM, ATTN: BENET WEAPONS LABORATORY, DRDAR-LCB-TL, WATERVLIET ARSENAL, WATERVLIET, N.Y. 12189, OF ANY REQUIRED CHANGES.

TECHNICAL REPORT EXTERNAL DISTRIBUTION LIST (CONT.)

	NO. OF COPIES
COMMANDER US ARMY RESEARCH OFFICE P.O. BOX 12211 RESEARCH TRIANGLE PARK, NC 27709	1
COMMANDER US ARMY HARRY DIAMOND LAB ATTN: TECH LIB 2800 POWDER MILL ROAD ADELPHIA, MD 20783	1
DIRECTOR US ARMY INDUSTRIAL BASE ENG ACT ATTN: DRXPE-MT ROCK ISLAND, IL 61299	1
CHIEF, MATERIALS BRANCH US ARMY R&S GROUP, EUR BOX 65, FPO N.Y. 09510	1
COMMANDER NAVAL SURFACE WEAPONS CEN ATTN: CHIEF, MAT SCIENCE DIV DAHLGREN, VA 22448	1
DIRECTOR US NAVAL RESEARCH LAB ATTN: DIR, MECH DIV CODE 26-27 (DOC LIB) WASHINGTON, D.C. 20375	1 1
NASA SCIENTIFIC & TECH INFO FAC P.O. BOX 8757, ATTN: ACQ BR BALTIMORE/WASHINGTON INTL AIRPORT MARYLAND 21240	1

	NO. OF COPIES
COMMANDER DEFENSE TECHNICAL INFO CENTER ATTN: DTIA-TCA CAMERON STATION ALEXANDRIA, VA 22314	12 (2-LTD)
METALS & CERAMICS INFO CEN BATTELLE COLUMBUS LAB 505 KING AVE COLUMBUS, OHIO 43201	1
MECHANICAL PROPERTIES DATA CTR BATTELLE COLUMBUS LAB 505 KING AVE COLUMBUS, OHIO 43201	1
MATERIEL SYSTEMS ANALYSIS ACTV ATTN: DRXSY-MP ABERDEEN PROVING GROUND MARYLAND 21005	1

NOTE: PLEASE NOTIFY COMMANDER, ARRADCOM, ATTN: BENET WEAPONS LABORATORY, DRDAR-LCB-TL, WATERVLIET ARSENAL, WATERVLIET, N.Y. 12189, OF ANY REQUIRED CHANGES.